Renormalisation equations for the two-dimensional Coulomb gas: inclusion of the single-particle charge distribution and comparison with Monte Carlo simulations

1990 J. Phys.: Condens. Matter 2 2345

(http://iopscience.iop.org/0953-8984/2/10/002)

J. Phys.: Condens. Matter 2 (1990) 2345–2354. Printed in the UK

Renormalisation equations for the two-dimensional Coulomb gas: inclusion of the single-particle charge distribution and comparison with Monte Carlo simulations

Vittorio Cataudella, Petter Minnhagen and Hans Weber
Department of Theoretical Physics, Umeå University, 901 87 Umeå, Sweden

Received 6 September 1989

Abstract. A set of self-consistent equations for the high-temperature phase of the two-dimensional Coulomb gas is solved numerically. These equations explicitly include the charge distribution of a single particle. Comparisons are made with Monte Carlo simulations as well as with the 'point-charge'-limit of the equations. The results are discussed in the context of type II superconducting films.

1. Introduction

The two-dimensional Coulomb gas is the prototype for a system undergoing a Kosterlitz–Thouless transition. Another interesting aspect of this model is that it describes vortex fluctuations for superfluid and superconducting films and, in this respect, is directly accessible to experiments [1].

Two methods have so far been used in order to obtain information on the Coulomb gas model; one is through solving renormalisation type equations and the other is through Monte Carlo simulations [1]. In the present paper we investigate a particular set of renormalisation equations for the Coulomb gas [2, 3, 4] and compare the result with Monte Carlo simulations. In earlier work on these renormalisation equations the point charge limit of the equations was studied [2, 3, 4]. This means that the charge distribution of a single particle was not explicitly taken into account. The point charge limit may be expected to give the general gross properties of the model [3]. In the present investigation we extend the earlier work and include the single-particle charge distribution.

In the case of vortex fluctuations for superfluid and superconducting films a vortex corresponds to a particular Coulomb gas single-particle charge distribution [1, 5]. A specific description which takes this into account on the level of a phenomenological Ginzburg–Landau theory is the Ginzburg–Landau Coulomb gas model [1, 5]. Monte Carlo simulations indicate that this model gives a good description of the resistive tail for type II superconducting films [1, 6]. The explicit shape of the single-particle charge distribution plays a crucial role in establishing this agreement [6]. The fact that, in this context, the single-particle charge distribution is an essential part of the physics is one of the motivations for the present study. We have concentrated our study on the high-temperature phase of the Coulomb gas because it is in this regime that we are able to perform Monte Carlo simulations.

0953-8984/90/102345+10$03.50

A description of the Coulomb gas as well as of the approximation scheme which is the starting point of the present paper are contained in [3] and will not be repeated here. Reference [3] will in the following be referred to as paper I.

In section 2 we introduce some notation and describe the basic equations. The solutions including the single-particle charge distribution are compared to the corresponding point charge limit solution in section 3. A comparison with Monte Carlo simulations are given in section 4, while section 5 contains some concluding remarks.

2. The basic equations

The two-dimensional Coulomb gas consists of particles which have positive or negative charge $s = \pm 1$, where the charge of each particle is distributed accordingly to a single-particle charge distribution $f(r)$. The interaction between two charges $s^2 U(r)$ is

$$U(r) = \int \mathrm{d}\boldsymbol{r}' f(r') V(|\boldsymbol{r} - \boldsymbol{r}'|) \tag{1}$$

where $V(r)$ is defined by the Poisson equation

$$\nabla^2 V(r) = -2\pi f(r) \tag{2}$$

In the point charge limit ($f(r) \to \delta(r)$) equations (1) and (2), in two dimensions, give $U(r) \sim -\ln r$. The Coulomb gas model is defined by the partition function Z corresponding to a grand canonical ensemble

$$Z = \sum_{N=0}^{\infty} \left[\frac{1}{(N/2)!}\right]^2 \int \mathrm{d}\boldsymbol{r}_1 \ldots \mathrm{d}\boldsymbol{r}_N \frac{1}{\Delta^N} \exp(-H_N/T) \tag{3}$$

where

$$H_N = \frac{1}{2} \sum_{i \neq j} s_i s_j [U(|\boldsymbol{r}_i - \boldsymbol{r}_j|) - U(0)] - N\mu. \tag{4}$$

Here μ is the chemical interaction, Δ is the phase space division, N is the number of particles in a configuration, T is the temperature, the index i numerates the particles and $s_i = \pm 1$ is the charge of particle i. The system is neutral so that there are equally many positive and negative particles in each configuration. For fixed single-particle function $f(r)$ and phase space division Δ, the thermodynamic properties of this model is a function of the chemical interaction μ and the temperature T. (Our unit system is chosen such that $k_B = 1$ and $s^2 = 1$).

Our aim is to study the high-temperature phase of this system with special emphasis on the effect of the single-particle charge distribution. The approximation scheme, which we will use, has been developed in paper I and we refer to this paper for details. Here we will only sketch the general approach and describe the basic equations.

The fundamental idea is to obtain an equation for the linearly screened interaction, $U_l(r)$. From the linearly screened interaction we obtain two key quantities characterising the system i.e. the screening length λ and the dielectric constant ϵ_a. These quantities are related to the small k-limit of the linearly screened interaction by

$$\hat{U}_l(k) = \frac{1}{\epsilon_a} \frac{2\pi}{k^2 + \lambda^{-2}} \qquad k \to 0. \tag{5}$$

The screening length λ is infinite in the low-temperature phase and finite in the high-temperature phase [1]. Furthermore the quantity $\epsilon_a T\lambda^{-2}/2\pi$ gives an estimate of the density of free charges, n_f, present in the high-temperature phase [1]. The density of free charges is through the Bardeen–Stephen formula [7] directly related to the resistive tail of superconducting type II films [1].

By using standard linear response theory we can write $U_1(r)$ in terms of the inverse dielectric function, or, equivalently, in terms of the density–density correlation function $g(r) = \langle \Delta n(r) \Delta n(0) \rangle$

$$U_1(r) = -\int \mathrm{d}r' f(|r-r'|) \int \mathrm{d}r'' \epsilon^{-1}(|r'-r''|) \int \mathrm{d}r''' \ln(|r''-r'''|) f(r''') \tag{6}$$

where

$$\epsilon^{-1}(|r'-r''|) = \delta(|r-r''|) + \beta \int \mathrm{d}r_0 \ln(|r'-r_0|) \langle \Delta n(r_0) \Delta n(r'') \rangle \tag{7}$$

in which Δn is the charge density

$$\Delta n(r) = \sum_{i=1}^{N} s_i f(|r-r_i|)$$

β in equation (7) is equal to $1/T$.

It was shown in paper I that it is possible to expand the density–density correlation function $g(r)$ in terms of the interaction $U_1(r)$. This leads to a systematic approximation scheme for $U_1(r)$ (see paper I for details). To lowest order in this approximation scheme we obtain

$$g(r_0) = -\frac{4z^2}{\Delta^2} \mathrm{e}^{-\beta U_1(0)} \int \mathrm{d}r'' \left[F(|r_0 - r''|) - F(r_0) \right] \sinh[\beta U_1(r'')] \tag{9}$$

where

$$F(r) = \int \mathrm{d}r' f(r') f(|r-r'|)$$

and we have, following the convention, introduced the fugacity variable $z = \exp(\beta\mu)$ instead of the chemical potential μ.

Equations (6), (7) and (9) together constitute a non-linear integral equation. This is the basic equation of the present paper.

In principle, it is possible to improve the approximation by including further terms in the expansion for $g(r_0)$ but, unfortunately, the complexity of the equation makes them intractable. In order to estimate the contribution from the next order of approximation, we have instead inserted the solution of lowest order equations into the next order equations which means that we in this estimate sacrifice the full self-consistency of the solution (see appendix and paper I).

3. Comparison with the point charge case

In the present investigation we have chosen the single-particle charge distribution

$$f(r) = \frac{1}{\pi b^2} e^{-(r/b)^2} \tag{11}$$

We made this choice for simplicity and in view of the fact that Monte Carlo simulations [6] suggest a small sensitivity to the more detailed shape. The constant b may be determined so as to obtain the best agreement with some explicit physical realisation. For example, $b = 2\xi$ corresponds to the shape calculated from the Ginzburg–Landau equations where ξ is the Ginzburg–Landau coherence length [5]. (This last result is obtained by minimising the Ginzburg–Landau equations with b as a variational parameter.)

With $f(r)$ given by equation (11) we obtain by combining with equations (6) and (9)

$$U_1(r) = -\left(\frac{2\bar{z}\pi}{b^2}\right)^2 \beta e^{-\beta U_1(0)} \int_0^\infty dr' \, L(r,r') \sinh(\beta U_1(r')) \tag{12}$$

where

$$L(r,r') = r' \int_0^\infty dr'' \, r'' \tilde{F}(r,r'') \int_{r''}^\infty dr''' \, K_0(r'',r''')[\tilde{F}(r''',r') - 2\pi F(r''')] \tag{13}$$

and

$$K_0(r,r') = r'^3 \left[1 - \left(\frac{r}{r'}\right)^2 - \ln\frac{r'}{r}\left(1 + \left(\frac{r}{r'}\right)^2\right)\right] \tag{14}$$

$$b^2\tilde{F}(r,r') = \exp[(r^2 + r'^2)/2b^2] I_0(rr'/b^2) \tag{15}$$

$$2\pi b^2 F(r) = \exp(-r^2/2b^2) \tag{16}$$

Here $I_0(r)$ is the modified Bessel function of the first kind and we have introduced the fugacity variable $\bar{z} = zb^2/\Delta$.

A main difference with the point charge case is that the kernel $L(r,r')$, in the present case, is well defined everywhere. Or, in other words, the single-particle charge distribution removes the singularity at $r = 0$ of the interaction $U_1(r)$ which is present in the point charge limit [3].

In order to solve equation (12) and establish the link between the interaction and the screening length λ, we proceed in the following way. First we note that equation (12), for large r, becomes a linear equation which can be solved in a closed form. The solution of this linear equation U_1^0 can be found straightforwardly in the Fourier space, i.e.

$$\hat{U}_1^0(k) = \frac{2\pi\hat{F}(k)}{k^2 + B\hat{F}(k)} \tag{17}$$

where $B = (4\pi\bar{z})/b^2 T \exp(-\beta U_1(0)/2)$. Since both the complete self-consistent equation and the linear solution, in k-space, are of the general form [1]

$$\hat{U}_1(k) = \frac{1}{\epsilon_a} \frac{2\pi\hat{F}(k)}{k^2 + \lambda^{-2} + \sum_{n=2} A_n k^{2n}} \tag{18}$$

we get, by comparison with equation (17)

$$B = \epsilon_a \lambda^{-2} \qquad \epsilon_a = (1 + b^2/2\lambda^2)^{-1}. \tag{19}$$

Equation (19) also provides a precise definition of λ (compare equation (5)).

By using (19) in equation (12), we finally get an equation for $\beta U_1(r)$ for each fixed value of λ, which we solve by standard numerical means. From these solutions and by aid of the relation

$$T = -\pi^2 \int_0^\infty r^3 g(r)\, dr \tag{20}$$

we construct a family of curves in the $(\bar{z}, T)$ plane where each curve corresponds to a fixed value of λ. Equation (20) reflects the fact that the inverse of the dielectric function in k-space at $k = 0$ must vanish in the high-temperature phase [1].

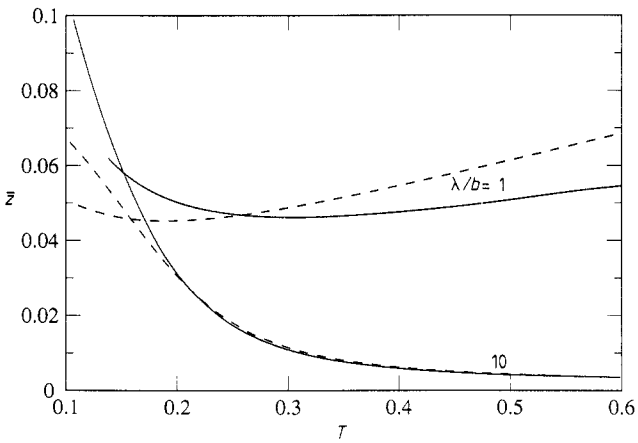

Figure 1. Comparison between the lowest order approximation (including the single-particle charge distribution) and the point charge limit of the same approximation [3]. The curves are trajectories for constant λ/b in the $(\bar{z}, T)$ plane. Full curves include the single-particle charge distribution and broken curves correspond to the point charge limit [3]. The upper and lower sets of curves correspond to $\lambda/b = 1$ and $\lambda/b = 10$, respectively.

In figure 1 we compare the calculated curves (i.e. the curves in the $(\bar{z}, T)$ plane for fixed λ/b) to the corresponding ones for the point-charge case [3]. As seen in the figure there are no appreciable differences for large values of λ/b and T (see the $\lambda/b = 10$ curves for $T \geq 0.2$) while for smaller values of λ/b the differences are quite large (see the $\lambda/b = 1$ curves). This can be understood in the following way: A large value of λ/b and a high T means a small particle density of which only a small fraction are bound in neutral pairs [1]. Consequently, the particles are on the average far apart and do not probe each others single-particle distribution. Hence the point charge limit of the equations becomes a good approximation. A smaller value of λ/b, on the other hand, means a larger particle density and the particles are closer on the average and will, because of this probe, each others charge distribution and as a consequence the point charge limit becomes inadequate.

In the comparison given in figure 1 we have optimised the correspondence between the point charge limit and the solution in the present paper in the following way: The

small distance cut-off of the integrals in the point charge limit is r_0 so that the 'point charge' curves in figure 1 correspond to constant λ/r_0 [3]. Roughly speaking both r_0 for the point charge case and b for the single-particle disribution given by equation (11) corresponds to the size of a charge. We have chosen $r_0 = b$ in the comparison. This choice ensures that the point charge solution and the one which includes the single-particle distribution given by equation (11) have the same 'large T small$\bar{z}$'-limit $(\lambda/b)^{-2} = 4\pi\bar{z}/T$. This means that in this limit the curves in figure 1 for the two solutions will merge.

The fact that the comparisons in figure 1 does not extend down to $T = 0$ is just a technical difficulty: our numerical solution of equation (12) becomes numerically instable for small T, presumably reflecting the existence of the low-temperature phase.

4. Comparison with Monte Carlo simulations

Another way of obtaining information on the two-dimensional Coulomb gas is through Monte Carlo simulations. A computer code which simulates the two-dimensional Coulomb gas with a single-particle charge distribution (like the one in equation (11)) has been developed earlier in [6] and we refer to this work for details.

The object of the Monte Carlo simulations in [6] was to establish a link between the resistive tail for type II superconducting films and the Ginzburg–Landau Coulomb gas model [5]. The key quantity in this context is $\epsilon_a\lambda^{-2}$, or in other words, the first moment of the linearly screened interaction $U_1(r)$ (compare equation (5)). This quantity is through the Bardeen–Stephen formula directly related to the resistance of superconducting type II films [1]. A suggestive agreement between resistance data and the Ginzburg–Landau Coulomb gas model was found through this connection [6].

In the present section we will compare the quantity $\epsilon_a\lambda^{-2}$ from the Monte Carlo simulations with the calculation of the same quantity from the lowest order equations and the (estimated) next order correction in our approximation scheme (see section 2 and the appendix).

In principle the Monte Carlo simulations correspond to including all orders in our approximation scheme. Thus a comparison of the Monte Carlo results with the results from the low order terms in our expansion tests the convergence and the validity of the expansion. However, one must also bear in mind that the Monte Carlo simulations by themselves are not completely exact. The reason for this is the following: The starting point for the Monte Carlo code developed in [6] is a mathematically exact formulation of the two-dimensional Coulomb gas with a single-particle charge distribution in terms of a non-local sine-Gordon field theory. The continuous field in this formulation is discretised and put on a lattice. The Monte Carlo simulations are by necessity performed on a lattice of finite size. Thus a possible source for deviations from the exact result can be associated with the finite lattice and the representation of the single-particle charge distribution on a finite lattice. Nevertheless, the results of [6] suggest that the lattice sizes and the representation of the single-particle charge distribution used in the simulations give results close to the exact ones. Our present comparisons give an additional test of this because a good agreement between the approximation scheme and the Monte Carlo simulations for high temperatures (where the lowest order approximation becomes exact [3]) may be taken as a verification.

The Monte Carlo simulation results in the present paper correspond to the lattice size 16×16 with periodic boundary conditions. The single-particle charge distribution

was represented as in ([6]) by five squares where the total charge over the central square was chosen as $p_0 = 5/12$. These choices were in ([6]) found to be close to optimal and we refer the reader to this previous work for further details. The choices made correspond to the ratio $b/a = 0.83$ where b is the extent of the single-particle distribution given by equation (11) and a is the lattice distance for the lattice discretising the continuous field in the sine-Gordon formulation.

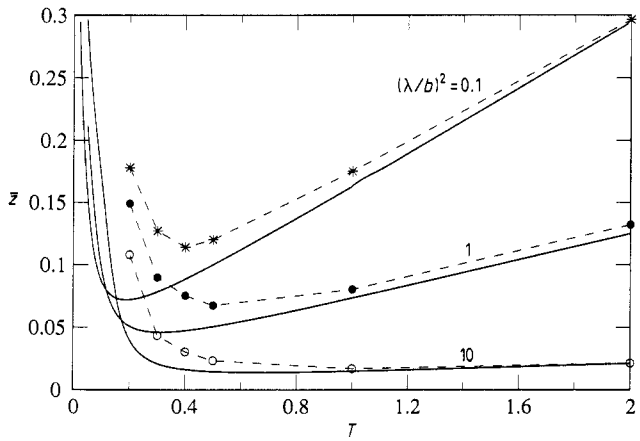

Figure 2. Comparison between the lowest order approximation (including the single-particle charge distribution) and Monte Carlo simulations. The full curves are trajectories for constant λ/b in the $(\bar{z}, T)$ plane obtained from the lowest order approximation. From top to bottom they correspond to $(\lambda/b)^2 = 0.1$, 1 and 10. The asterisks, full circles, and open circles are obtained from Monte Carlo simulations and should be compared to the $(\lambda/b)^2 = 0.1$, 1 and 10 curves, respectively. The broken lines are just a guide to the eye.

The comparisons are shown in figures 2 and 3. The full curves in figure 2 are 'constant λ/b' curves in the $(\bar{z}, T)$ plane obtained from the lowest order approximation (given by equation (12)). From top to bottom in the figure they correspond to $(\lambda/b)^2 = 0.1$, 1 and 10, respectively. The asterisks, full circles and open circles are results from the Monte Carlo simulations. The asterisks, full circles, and open circles should be compared to the $(\lambda/b)^2 = 0.1$, 1 and 10 curves, respectively. We are comparing the results for the quantity $\epsilon_a(\lambda/b)^{-2}$. This means that an open circle corresponds to the same value of $\epsilon_a(\lambda/b)^{-2}$ as the point vertically below on the lowest order $(\lambda/b)^2 = 10$ curve (and similarly for the full circles and asterisks).

As seen in figure 2 the Monte Carlo simulations are for $T \geq 1$ in excellent agreement with the lowest order calculation. This is in accord with the theoretical expectations because the lowest order calculation becomes exact in the limit of high temperatures [3]. As discussed in the previous section, the difference between the $\lambda/b = 1$ curves in figure 1 is an effect of the single-particle charge distribution; the particles are so close that they probe each others single-particle distribution. Hence the agreement for $T \geq 1$ between the $(\lambda/b)^2 = 1$ curve and the corresponding Monte Carlo results shown in figure 2 verifies that the lattice size and the representation of the single-particle charge distribution used in the Monte Carlo simulations are indeed quite adequate. This conclusion is further enforced by the agreement between the $(\lambda/b)^2 = 0.1$ curve and the corresponding Monte Carlo results because the particles are on the average even closer in this case. It follows that the discrepancy between the

lowest order calculation and the Monte Carlo simulations for $T < 1$ to large extent can be attributed to the neglect of the higher order terms in our expansion. It then also follows that the higher order terms becomes more important for smaller temperatures. Nevertheless, the qualitative features are well represented already by the lowest order calculation. The only qualitative difference is the crossing of the curves from the lowest order calculation occuring at the smallest temperatures. As discussed in paper I such crossings reflect the mean field character of the lowest order calculation and signals a phase transition. The signal of such a phase transition for the exact solution would be the merging at small temperatures of curves corresponding to a some continuous range of λ/b values. However, the convergence and the resolution of our Monte Carlo program are not high enough to resolve such a feature.

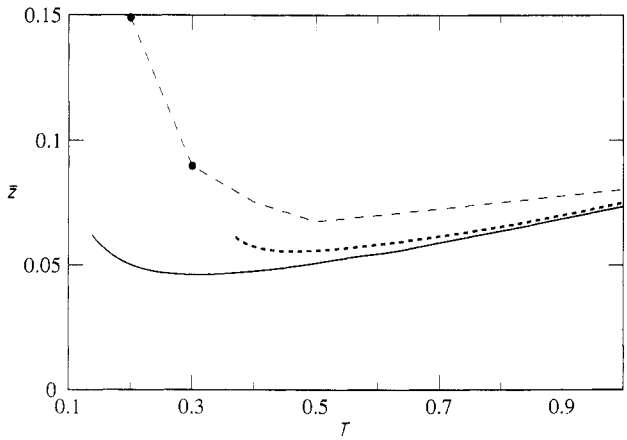

Figure 3. Comparison of the $\lambda/b = 1$ trajectory in the $(\bar{z}, T)$ plane obtained from the lowest order approximation (including the single-particle charge distribution) (full curve), the (estimated) next order (dotted curve) contribution, and Monte Carlo simulation (full circles). The broken lines are just a guide to the eye.

Figure 3 shows a comparison between the $\lambda/b = 1$ curve from the lowest order calculation (full curve), the $\lambda/b = 1$ curve from the calculation including the (estimated) next order correction (broken curve, see the appendix for a description of the correction term), and the Monte Carlo simulations (full circles). As expected the next order correction comes much closer to the Monte Carlo results. However, the remaining discrepancy suggests that one would have to include a few more orders in our expansion in order to get a good approximation of the exact result for $T < 1$. Such a calculation would be quite intractable.

The connection between the 'universal resistance' curve for superconducting type II films [1] and the Coulomb gas quantity $\epsilon_a \lambda^{-2}$ was in [6] established for the Coulomb gas temperature interval $0.3 \leq T \leq 0.6$ and $0.1 \leq \epsilon_a (\lambda/b)^{-2} \leq 1$. As is apparent in figure 3 the higher order terms are in this temperature range quite important. This suggests that it would in fact be very difficult to calculate the 'universal resistance' curve [1] without resorting to Monte Carlo simulation.

5. Concluding remarks

In the present paper we have investigated the importance of the single-particle charge

distribution for the properties of the two-dimensional Coulomb gas.

It was explicitly demonstrated that, when the particles are close enough on the average, the single-particle charge distribution is an essential part of the physics. This conclusion carries over to the the description of the resistive tail for superconducting type II films; the shape of the universal resistance curve [1] contains information of the vortex core. Or, in other words, a point charge type description is not adequate for the universal resistance curve. In principle, a point charge description would be appropriate close enough to the critical temperature for an infinite sample [1]. However, it is not clear whether this critical region can ever be resolved in practice due to finite size effects and other experimental limitations [1]. The fact that the single-particle charge distribution has to be included in order to calculate the universal resistance curve was reached in earlier Monte Carlo simulation work [6]. The present investigation corroborates this conclusion. It also verifies that the approximation of the single-particle charge distribution used in the earlier Monte Carlo simulation work is indeed adequate.

It was also demonstrated by comparing to Monte Carlo results that the key quantity in the connection to superconducting films, $\epsilon_a(\lambda/b)^{-2}$, can be calculated from a systematic approximation scheme developed earlier [3]. Already the lowest order of this approximation scheme gave all the essential qualitative features. However, we also concluded that the calculation of the universal resistance curve would require a few more orders in this expansion scheme. Such a calculation was deemed to be extremely cumbersome. This suggests that it would be very hard to calculate the universal resistance curve without resorting to Monte Carlo simulations. This reflects the fact that the universal resistance curve does not correspond to any critical properties of the two-dimensional Coulomb gas.

The limitations of the numerical convergence of the present calculation prevented an investigation of the phase transition lines for the two-dimensional Coulomb gas. However, the present calculations suggest that the actual location of the phase transition lines in the $(\bar{z}, T)$ plane will be quite sensitive to the shape of the single-particle charge distribution.

Acknowledgments

This work was supported by the Swedish Natural Science Research Council. We are grateful to Mats Wallin for proving the numerical data for the point charge case.

Appendix

Equation (9) is the lowest order approximation of the charge-density correlation function $g(r)$ in terms of the linearly screened interaction $U_1(r)$. Including the next order correction in this expansion gives (see paper I)

$$g(r) = \frac{2z_{\text{eff}}^2}{b^2} \int \mathrm{d}\boldsymbol{r}' \, [F(|\boldsymbol{r} - \boldsymbol{r}'|) - F(\boldsymbol{r})]\{\exp[-\beta(U_1(\boldsymbol{r}') + \tfrac{1}{4}A^{++}(\boldsymbol{r}'))] - \exp[\beta(U_1(\boldsymbol{r}') - \tfrac{1}{4}A^{+-}(\boldsymbol{r}'))]\} \tag{A1}$$

where

$$\tfrac{1}{4}A^{++}_{+-}(r) = \frac{2z_{\text{eff}}}{\beta b^2}\int \mathrm{d}r' \left(\cosh[\beta(U_1(|r-r'|) \pm U_1(r'))] - \frac{\beta^2}{2}[U_1(|r-r'|) \pm U_1(r')]^2 - 1\right) \tag{A2}$$

and $z_{\text{eff}} = \bar{z}\exp[-\beta U_1(0)/2]$.

The self-consistent solution of the equation set given by equations (6), (7), (A1), and (A2) gives U_1 to the next order. This next order $U_1(r)$ reduces to the lowest order solution for large r (see paper I). This means that the 'constant λ/b' curves in the $(\bar{z}, T)$ plane can again be calculated by aid of equations (19) and (20). However, it turns out to be numerically cumbersome to solve equations (6), (7), (A1), and (A2) .

As an alternative, we have in the present investigation estimated the next order correction to the lowest order approximation by inserting the lowest order solution directly into equations (A1) and (A2). We then replace the true next order $g(r)$ (corresponding to full self-consistency) by the $g(r)$ obtained in this way. The corresponding U_1 is then obtained by aid of equations (6) and (7). The lack of self-consistency causes this estimate to break down for temperatures that are too low, but for higher temperatures it ought to be a good estimate of the next order correction.

References

[1] For a general review see, e.g.,
Minnhagen P 1987 *Rev. Mod. Phys.* **59** 1001
[2] Minnhagen P 1985 *Phys. Rev. Lett.* **54** 2351; 1985 *Phys. Rev.* B **32** 3088
Minnhagen P and Wallin M 1987 *Phys. Rev.* B **36** 5620
[3] Minnhagen P and Wallin M 1989 *Phys. Rev.* B **40** 5109
[4] Thijssen J M and Knops H J F 1988 *Phys. Rev.* B **38** 9080
[5] Minnhagen P and Nylén M 1985 *Phys. Rev.* B **31** 5768
[6] Minnhagen P and Weber H 1985 *Phys. Rev.* B **32** 3337
Weber H and Minnhagen P 1988 *Phys. Rev.* B **38** 8730
[7] Bardeen J and Stephen M J 1965 *Phys. Rev.* **140A** 1197